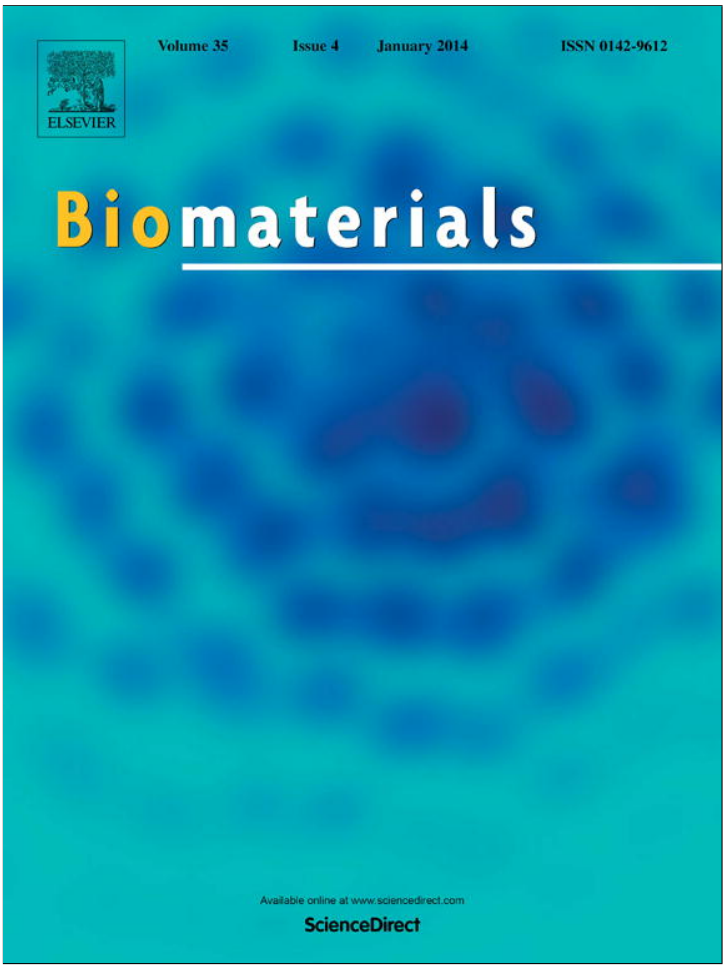

Biomaterials 35 (2014) 1205–1214

Contents lists available at ScienceDirect

Biomaterials

journal homepage: www.elsevier.com/locate/biomaterials

Electrospun gelatin scaffolds incorporating rat decellularized brain extracellular matrix for neural tissue engineering

Silvia Baiguera [a,1], Costantino Del Gaudio [b,1], Elena Lucatelli [b], Elena Kuevda [c], Margherita Boieri [d], Benedetta Mazzanti [d], Alessandra Bianco [b], Paolo Macchiarini [a,*]

[a] Advanced Center for Translational Regenerative Medicine (ACTREM), Karolinska Institutet, Stockholm, Sweden
[b] University of Rome "Tor Vergata", Department of Industrial Engineering, Intrauniversitary Consortium for Material Science and Technology (INSTM) Research Unit Tor Vergata, Rome, Italy
[c] International Scientific-Research Clinical and Educational Center of Regenerative Medicine, Kuban State Medical University, Krasnodar, Russian Federation
[d] Department of Clinical and Experimental Medicine, University of Florence, Florence, Italy

ARTICLE INFO

Article history:
Received 29 July 2013
Accepted 20 October 2013
Available online 8 November 2013

Keywords:
Cytocompatibility
Decellularized brain extracellular matrix
Neural tissue engineering
Mesenchymal stromal cell differentiation

ABSTRACT

The fabrication of an instructive bioabsorbable scaffold is one of the main goals for tissue engineering applications. In this regard, genipin cross-linked gelatin scaffolds, produced by electrospinning, were tested as a platform to include decellularized rat brain extracellular matrix as an active agent to provide fundamental biochemical cues to the seeded cells. This approach is expected to furnish a suitable natural-based polymeric scaffold with sufficient temporal stability to support cell attachment and spreading, also providing tissue-specific signals that can contribute to the expression of the requested cellular phenotype. We first demonstrated the effectiveness of the proposed decellularization protocol and the cytocompatibility of the resulting brain matrix. Then, the *in vitro* biological assays of the conditioned electrospun scaffolds, using rat allogeneic mesenchymal stromal cells, confirmed their biocompatibility and showed a differentiative potential in presence of just 1% w/w decellularized rat brain extracellular matrix.

1. Introduction

The natural extracellular matrix (ECM), being a complex mixture of structural and functional proteins, can be considered as an inductive means for the development of active tissue engineered scaffolds [1]. This approach might lead to a potential alternative for the treatment of critical affections like those related to the central nervous system (CNS), that, due to the failure of neural regeneration, can result in permanent disability [2]. The development of an effective neural therapeutic strategy is of fundamental relevance since neurological, neurosurgical and psychiatric diseases account for one-third of the burden of all diseases in the developed world [3]. Loss of cells and tissue disrupt the normal brain architecture, inhibiting tissue regeneration, mainly due to a lack of matrix and structural support [4,5]. Indeed, it has been demonstrated that the interaction of cells, either transplanted or migrating endogenous stem cells, with the ECM plays a key role in brain healing and regeneration [6–10]. There is, therefore, a great need to develop new tools to reconstitute the native ECM and the tissue architecture of the damaged CNS. For this aim, it is necessary to bridge the tissue gap and provide supporting substrates. It should be considered that the cerebral ECM has a unique composition as it contains relatively small amounts of fibrous proteins, such as collagen, laminin and fibronectin, and high amounts of linear polysaccharides, such as glycosaminoglycans [11,12]. Appropriate biomaterials, to be processed for mimicking a three-dimensional instructive microenvironment with specific biochemical cues, and promoting cell migration, adhesion and survival, could therefore enhance the success of neural implants [13].

In this regard, the present study proposes a genipin cross-linked gelatin electrospun scaffold incorporating rat decellularized brain extracellular matrix (dBECM) as a potential improvement for cell adhesion, proliferation and differentiation and, as a consequence, for nervous tissue regeneration. In order to provide a morphological contribution to the seeded cells, electrospinning was selected as a cost-effective technique to produce fibrous dBECM-gelatin mats. Based on the same technique, previous studies showed the ability to produce (*i*) electrospun adipose tissue-derived ECM for

* Corresponding author. Advanced Center for Translational Regenerative Medicine (ACTREM), Karolinska Institutet, Alfred Nobels Allé 8, Huddinge, SE-141 86 Stockholm, Sweden. Tel.: +46 760 503 213 (mobile); fax: +46 8 774 7907.
E-mail address: paolo.macchiarini@ki.se (P. Macchiarini).
[1] Contributed equally to the work.

0142-9612/$ – see front matter © 2013 Elsevier Ltd. All rights reserved.
http://dx.doi.org/10.1016/j.biomaterials.2013.10.060

adipose stem cell culture [14], (*ii*) hybrid mats composed of porcine urinary bladder matrix and poly(ester-urethane)urea [15], and (*iii*) hybrid mats by combining electrospun poly(ester-urethane)urea and electrosprayed dermal ECM hydrogel extracted from decellularized adult porcine dermis [16].

A complete evaluation of the effective decellularization of the rat brain was firstly provided. Then, the collected electrospun mats were characterized by means of scanning electron microscopy (SEM) and differential scanning calorimetry (DSC) before and after the cross-linking procedure; cytocompatibility was assessed by *in vitro* testing rat mesenchymal stromal cells.

2. Materials and methods

2.1. Materials

Gelatin powder (type A, from porcine skin, M_w ranging from 50,000 to 100,000), phosphate buffered saline (PBS), Triton X-100, deoxycholate, DNAsi, antibiotic and antimycotic solution, papain, sodium acetate, N-acetyl cysteine and EDTA were supplied by Sigma–Aldrich (Milan, Italy), while paraffin, glutaraldehyde, hamatoxylin and eosin (H&E) by Merck (Darmstadt, Germany). Movat pentachromic stain kit was supplied by Diapath (Bergamo, Italy), 4′-6-diamidino-2-phenylindole (DAPI) by Vector Laboratories (CA, USA) and sodium cacodylate buffer (pH 7.2) by Prolabo (Paris, France). Dulbecco's modified Eagle's medium with low glucose (DMEM-LG) was supplied by Gibco-Invitrogen (Milan, Italy), while fetal bovine serum (FBS) by Hyclone (SouthLogan, Utah, USA). Cell WASH (0.1% sodium azide in PBS), CD54-FITC, CD11b-FITC, CD90-PE, GFAP-Alexa Fluor 647 and isotype-matched mouse MAb were supplied by BD Pharmingen (San Jose, CA, USA), CD44-Alexa Fluor 647 by Biolegend (San Diego, CA, USA), while MHCII-FITC by eBioscience (San Diego, CA, USA). Acetic acid was supplied by Carlo Erba Reagenti (Arese (MI), Italy), Genipin by Wako Chemicals GmbH (Neuss, Germany) and Lympholyte-H by Cedarlane (Burlington, Ontario, Canada). Nucleic Acid Purification Lysis Solution was supplied by Applied Biosystems (Foster City, CA), PCR Tissue Homogenizing kit from PBI International (Milan, Italy) and Master Pure™ DNA Purification kit from Epicentre Biotechnologies (Madison, WI). Fastin™ elastin assay kit and Blyscan Glycosaminoglycan Assay kit were provided from Biocolor (Carrickfergus, UK).

All materials and reagents were used as received.

2.2. Study design

Male Brown Norway rats ($n = 25$) (Charles River Laboratories Italia S.r.l., Calco, Italy), weighing 230–320 g, were used as donors of brain tissues and bone marrow. All animals received care in compliance with the "Principles of laboratory animal care" formulated by the National Society for Medical Research and the "Guide for the care and use of laboratory animals" prepared by the Institute of Laboratory Animal Resources, National Research Council, and published by the National Academy Press, revised in 1996. The study was approved by the Animal Care and Use Committee and the Bioethics Committee of the University of Florence (Italy). Rats were individually housed and maintained at an environmental temperature of 25 ± 2 °C and on a 12/12 h light/dark cycle. Animals were acclimated for 7 days before experiments.

Whole brains were harvested from donor rats. Brains ($n = 15$) were used for structural (H&E and Movat staining), morphologic (scanning electron microscopy, SEM), matrix content (elastin and glycosaminoglycan quantification) and effectiveness of decellularization (DAPI staining, nuclear counting, DNA quantification) evaluation. Decellularized brains ($n = 3$) were used for *in vitro* cytocompatibility studies. Afterwards, brains ($n = 7$) were decellularized, completely dehydrated and used to condition the gelatin scaffolds. Femurs and tibiae were harvested from donor rats ($n = 10$) for bone marrow harvest and used for MSC ($n = 5$) and MNC ($n = 5$) isolation.

2.3. Decellularization process

After harvesting, brain tissues were stored in cold PBS, containing 1% antibiotic and antimycotic solution, and subsequently processed using a modification of a previously described detergent-enzymatic method (DEM) [17], to obtain a complete tissue decellularization without losing most of the brain matrix. Briefly, samples were frozen (at −80 °C) and thawed completely four times, incubated with Milli-Q water (72 h at room temperature), and then processed twice as follows: 1.0% Triton X-100 (60 min), water (30 min), 4.0% deoxycholate (60 min), water (30 min), 2000 KU DNAsi in 1 M NaCl (60 min) and water (30 min). All the decellularization steps were performed using agitated baths at 60 rpm. After the last washing step, brain samples were stored in PBS containing 1% antibiotic and antimycotic solution at 4 °C.

2.4. dBECM characterization

2.4.1. Histological analysis

Parts of brain samples (native and decellularized) were fixed for 24 h in 10% neutral buffered formalin solution in PBS (pH 7.4) at room temperature. They were washed in distilled water, dehydrated in graded alcohol, embedded in paraffin, and sectioned at 5 μm thickness. Adjacent sections were deparaffinized, rehydrated and stained with H&E to evaluate tissue decellularization and morphology. To evaluate the tissue morphology, each sample was also stained with the Movat pentachromic stain kit, according to the manufacturer's protocols.

2.4.2. Assessment of cellular content

To evaluate the remaining cells after DEM, adjacent sections (5 μm thickness) were deparaffinized, rehydrated and stained with DAPI, a fluorescent nucleic acid stain (VECTASHIELD Mounting Medium with DAPI; excitation wavelength 350 nm, emission wavelength 460 nm) for 30 min at room temperature in darkness, and analyzed by fluorescence microscopy.

2.4.3. DNA quantification

To assess DNA quantification within native and decellularized brain matrices, samples ($n = 3$ for each condition) were resuspended in 200 μl Nucleic Acid Purification Lysis Solution and homogenized using PCR Tissue Homogenizing kit in microcentrifuge tubes. DNA was isolated using Master Pure™ DNA Purification kit, which is based on a gentle salt-precipitation protocol to allow a rapid purification of nucleic acids, and successively stored at −80 °C. DNA (diluted 1:50) was quantified by measuring the absorbance in a BIORAD spectrophotometer (*SmartSpec™ Plus spectrophotometer, BIORAD, Milan, Italy*).

2.4.4. Scanning electron microscopy

To qualitatively evaluate decellularized matrix structure, brain (native and decellularized) matrices were fixed with 3% (v/v) glutaraldehyde in a buffered solution of 0.1 M sodium cacodylate buffer (pH 7.2). After rinsing in cacodylate buffer, specimens were dehydrated through an ethanol gradient, critical point dried, sputter coated with gold and observed by means of scanning electron microscopy (SEM; JCM-5000 NeoScope, Nikon).

2.4.5. Elastin content measurement

Insoluble elastin was extracted from native and decellularized samples ($n = 4$ for each condition) as soluble cross-linked polypeptide elastin fragments, using the hot oxalic acid extraction technique. Wet samples (mean weight 187 ± 65 mg and 145 ± 30 mg for native and decellularized samples, respectively) were mixed with oxalic acid (0.25 M) and boiled in a water bath for 1 h. The supernatant was collected by centrifugation, and the sediment was submitted to a second and third extraction under the same conditions. Soluble elastin content in the oxalic extracts was determined using the colorimetric Fastin™ elastin assay kit, based on a fastin dye reagent (5,10,15,20-tetraphenyl-21,23-pophrine tetrasulfonate), following the manufacturer's instructions. Briefly, samples were added with elastin precipitating reagent, incubated for 15 min and centrifuge. The Dye Reagent was then added to allow the formation of elastin-dye complex. After incubation (90 min) and centrifugation, the elastin-dye complex was dissolved by incubation with the dye dissociation reagent for 10 min. Absorbance was measured at 513 nm on a Epoch Microplate Spectrophotometer (*BioTek, VT, USA*). Replicate samples were averaged and corrected by subtracting the blank average, and elastin content was determined from a standard curve constructed using five concentrations (5–25 mg) of α-elastin. Final values were expressed as mg of elastin per wet weight.

2.4.6. Sulfated glycosaminoglycan content measurement

Native and decellularized samples ($n = 4$ for each condition) were digested with 0.2 mg/mL papain in 0.2 M phosphate buffer (pH 6.4) containing 0.1 M sodium acetate, 5 mM N-acetyl cysteine and 10 mM EDTA at 65 °C overnight. Total sulfated glycosaminoglycans (GAG) was quantified using the Blyscan Glycosaminoglycan Assay kit, based on 1,9-dimethyl-methylene blue binding, following the manufacturer's instructions. Briefly, samples were added with Blyscan dye reagent, incubated for 30 min and centrifuge. The insoluble GAG-dye complex was then dissolved by adding the dissociation reagent and incubated for 10 min. Absorbance was measured at 656 nm on a Epoch Microplate Spectrophotometer (*BioTek, VT, USA*). Replicate samples were averaged and corrected by subtracting the blank average, and GAG content was determined from a standard curve constructed using five concentrations (1–5 μg) of GAG. Final values were expressed as μg of GAG per dry weight.

2.5. Scaffold fabrication

dBECM was lyophilized and stored dry until use. dBECM powder (1% w/w with respect to gelatin) was firstly ultrasonicated for 10 min in a mixture of acetic acid/deionized water (9:1), then gelatin powder was added (14% w/v). Neat scaffold was prepared by dissolving gelatin at the same concentration in the same solvent mixture. The resulting solution was then poured into a glass syringe to be electrospun through a blunt tip metallic needle (18G) onto a metallic target in the following conditions: 12 kV applied voltage (Spellman, USA), 0.4 ml/h feed rate (KD Scientific, USA), and 10 cm needle-to-target distance.

All samples were vacuum dried for 48 h and stored in a desiccator.

2.6. Cross-linking procedure

Genipin was dissolved in ethanol at 0.5% w/v and cross-linking was carried out by soaking the electrospun gelatin mats, neat and dBECM loaded, into the alcoholic

solution for 3 days at 37 °C. Subsequently, the cross-linked scaffolds were rinsed in ethanol and dried at room temperature for 24 h.

2.7. Scaffold characterization

2.7.1. Morphological characterization

The microstructure of as-spun and cross-linked gelatin mats was investigated by means of scanning electronic microscopy (SEM; Leo-Supra 35). Samples were sputter coated with gold prior to examination. The average fiber diameter was determined from SEM micrographs by measuring about 50 fibers randomly selected (ImageJ, NIH).

2.7.2. Differential scanning calorimetry measurements

The thermal properties of the electrospun gelatin mats, before and after cross-linking, were measured by differential scanning calorimetery (DSC; Nestch DSC 200 PC). Runs were carried out at a scanning rate of 10 °C/min up to 250 °C in an inert environment.

2.8. Biocompatibility analysis

2.8.1. Cell isolation

Rats were euthanized, by an intraperitoneal barbiturate overdose of 150 mg/kg, and the hind limbs harvested. The femur and tibia were cleared of soft tissue and cut at the metaphyses. Bone marrow was flushed out with Hank's Balanced Salt Solution (HBSS).

Mesenchymal stromal cells (MSCs): MSCs were isolated from rat bone marrow by means of adhesion to cell culture flasks. Bone marrow was centrifuged, and the cell pellets seeded in 75 cm^2 flasks in complete medium (DMEM-LG, supplemented with 20% FBS and 1% Penicillin–Streptomycin). Flasks were incubated at 37 °C in a humidified atmosphere containing 5% CO_2. Half of the complete medium was changed after 1 week, and thereafter, the entire medium was changed every 3–4 days. After 14 days in culture, the cells that adhered to the flask were defined as MSCs passage 0. MSC P0 were incubated for 5–10 min at 37 °C with 0.05% trypsin–0.02% EDTA, harvested, washed, and resuspended in complete medium. Expansion of the cells was obtained with successive cycles of trypsinization and reseeding. MSCs cultured above passage 4 were used for the experiments.

Mononuclear cells (MNCs): Bone marrow was diluted with HBSS and MNCs isolated by density centrifugation in Lympholyte-H (density 1.077 g/mL). MNC layer was collected, washed and counted. MNCs were resuspended in DMEM-LG supplemented with 20% FBS and 1% Penicillin–Streptomycin, and immediately seeded on mats.

2.8.2. Cell characterization

Fibroblast–colony-forming units (CFU-F): the number of CFU-F was used as a surrogate marker for MSC progenitor frequency; 1.5×10^6 cells were plated in duplicate in 100 mm^2 Petri dishes. After 14 days, the dishes were fixed with methanol and stained with Giemsa; visible colonies formed by 50 or more cells were counted and reported as the number of CFU-F/10^6 seeded cells.

Flow cytometric evaluation: MSCs were analyzed for the expression of surface antigens using flow cytometry procedures. Washed cells were resuspended in flow cytometry buffer consisting of Cell WASH with 2% FBS. Aliquots (1.5×10^5 cells/100 μL) were incubated with the following conjugated MAb: CD54-FITC, CD44-Alexa Fluor 647, CD11b-FITC, MHCII-FITC, CD90-PE, GFAP-Alexa Fluor 647. Non-specific fluorescence and morphologic parameters of the cells were determined by incubation of the same cell aliquot with isotype-matched mouse MAb. All incubations were done for 15 min and, after incubation, cells were washed and resuspended in 100 μL of CellWASH; 7-AAD (7-Aminoactinomycin-D) was added in order to exclude dead cells from the analysis. Flow cytometric acquisition was performed by collecting 10^4 events on a FACS Calibur (488 nm Argon laser equipped; *Becton Dickinson, Milan, Italy*) and data were analyzed on dot-plot bi-parametric diagrams using Cell Quest Prosoftware (*Becton Dickinson*).

2.8.3. Cell culture on evaluated samples

Decellularized brain samples (5 × 5 mm), gelatin mats and dBECM-gelatin mats (5 × 5 mm) were sterilized by immersion in 100% v/v ethanol solution for 1 h, dried in laminar hood at room temperature and incubated overnight with HBSS at 37 °C in a humidified atmosphere containing 5% CO_2. MSCs or MNCs (0.5×10^6 cells/cm^2) were seeded on samples, in a 24-well microtiter plate, and cultured under standard conditions for 7 days. MSCs cultured on tissue culture plates were considered the control case.

2.8.4. Construct examination

In order to investigate the cellular adhesion and morphology, after 7 days incubation period, cellular constructs were washed with PBS, fixed for 24 h in 10% neutral buffered formalin solution (pH 7.4), washed with HBSS and stained with H&E or with DAPI. Some constructs were fixed with glutaraldehyde (3% (v/v) in a buffered solution of 0.1 M sodium cacodylate buffer), rinsed in cacodylate buffer, dehydrated, critical point dried, sputter coated with gold and observed by means of SEM (JCM-5000 NeoScope, Nikon). Moreover, samples were also embedded in paraffin, and sectioned at 5 μm thickness. Sections were stained with H&E and DAPI.

2.8.5. Phenotypic analysis

To evaluate the *in vitro* differentiation potential of gelatin cross-linked mats, rat MSCs, cultured on scaffolds, were analyzed for the expression of specific neural surface antigen (anti GFAP) using flow cytometry procedures. Rat MSCs seeded on culture plates were used as negative controls. After 7 days incubation period, MSCs were detached from scaffolds, washed and resuspended in flow cytometry buffer consisting of Cell WASH with 2% FBS. Aliquots (1.5×10^5 cells/100 μL) were incubated with the following conjugated MAb: CD54-FITC, CD44-Alexa Fluor 647, CD11b-FITC, MHCII-FITC, CD90-PE, GFAP-Alexa Fluor 647. Non-specific fluorescence and morphologic parameters of the cells were determined by incubation of the same cell aliquot with isotype-matched mouse MAb. All incubations were done for 15 min and, after incubation, cells were washed and resuspended in 100 μL of CellWASH; 7-AAD (7-Aminoactinomycin-D) was added in order to exclude dead cells from the analysis. Flow cytometric acquisition was performed by collecting 10^4 events on a FACS Calibur (488 nm Argon laser equipped; *Becton Dickinson, Milan, Italy*) and data were analyzed on dot-plot bi-parametric diagrams using Cell Quest Prosoftware (*Becton Dickinson*).

2.9. Statistics

Results are expressed as mean ± standard deviation. Significant differences were estimated by Mann–Whitney U test. p values less than 0.05 were considered significant.

3. Results

3.1. dBECM characterization

Brain tissue, treated with the modified decellularization process, was completely decellularized and no cells and nuclear material were detected by H&E and DAPI staining (Fig. 1A–D). Furthermore, DNA quantification showed that approximately 91% of the nuclear material was removed by the decellularization process (5.1 ± 0.2 ng/μl for native and 0.51 ± 0.02 ng/μl for decellularized samples), suggesting that decellularized brain matrices were significantly ($p < 0.05$) depleted of DNA contents. Moreover, Movat pentachromic staining showed that the three-dimensional architecture and the protein network of the dBECM remained intact and unaltered (Fig. 1E, F), which was confirmed by scanning electron microscopy (Fig. 1G, H). Additionally, dBECM showed a similar elastin (per wet weight) and sulfated glycosaminoglycan (per dry weight) content with respect to native samples (Fig. 1I, J). Results suggested that the decellularization protocol allowed to obtain a brain acellular matrix that retains the micro- and ultra-structural details of brain architecture, without losing most of the brain matrix, yet completely removing cellular components.

Decellularized brain matrices allowed MSC adhesion, proliferation and ingrowth: H&E and DAPI staining of seeded dBECM showed, indeed, the presence of MSCs not only on the external surface, where cells have been seeded, but also in the inner part of the decellularized samples (Fig. 2).

3.2. Electrospun mats

3.2.1. Morphological evaluation

The morphology of electrospun gelatin fibers was assessed by means of SEM analysis. The collected neat mats were characterized by a random arrangement of fibers, free of defects, with an average diameter of 200 ± 70 nm (Fig. 3A). Similarly, dBECM-gelatin mats were made of uniform fibers with an average diameter of 320 ± 70 nm (Fig. 3C).

Genipin cross-linked mats were successfully obtained: the fibrous structure was retained even if slight modifications occurred as compared to the respective as-spun cases, highlighting restricted fused regions where fibers overlapped (Fig. 3B, D). Average fiber diameters were 570 ± 140 nm and 800 ± 180 nm for neat and dBECM-gelatin mats, respectively ($p < 0.05$ for both cases compared to the related uncross-liked ones).

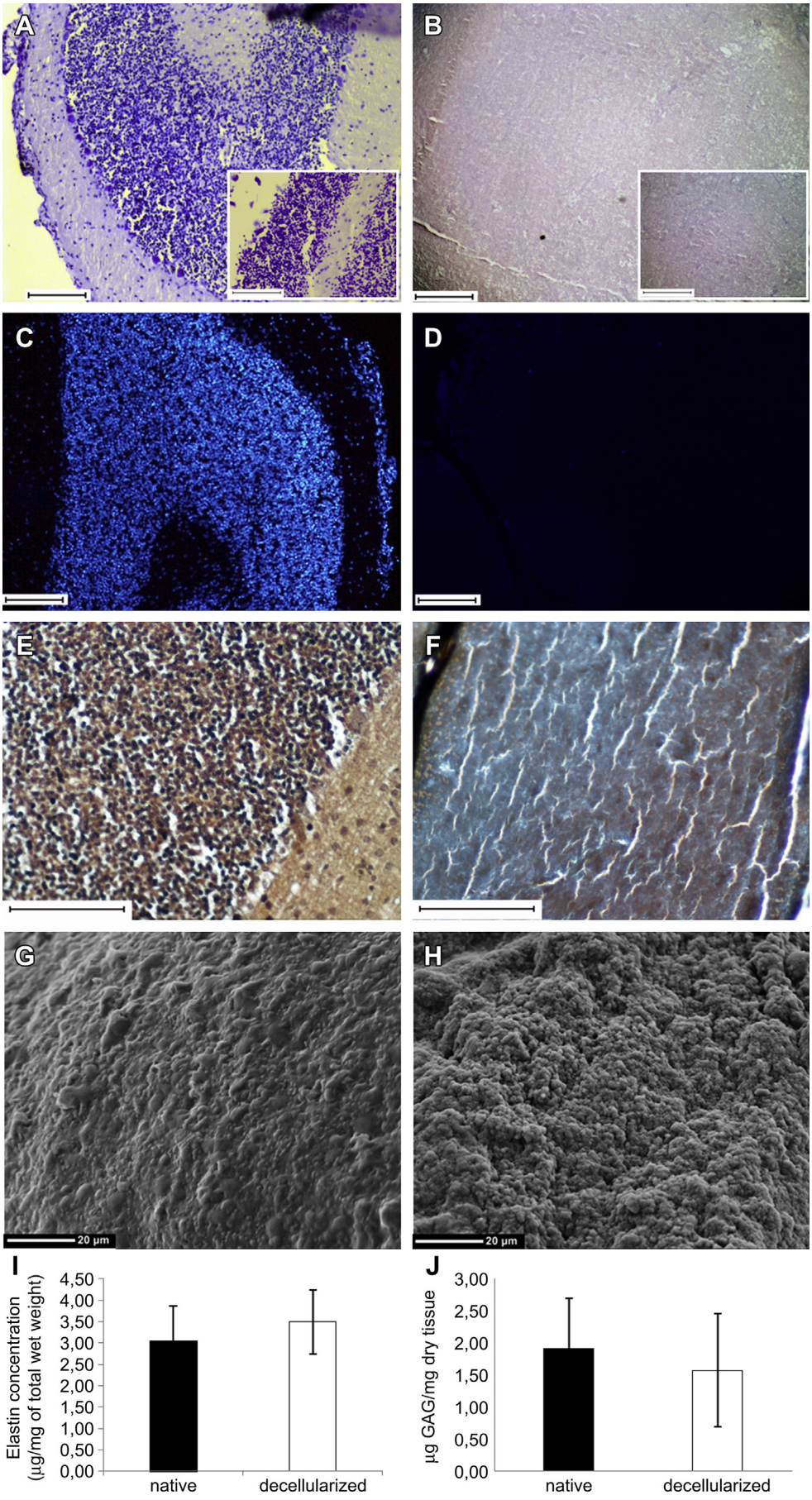

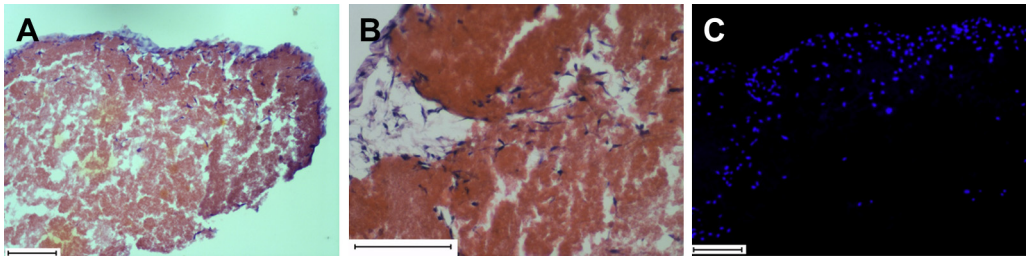

Fig. 2. Hematoxylin and eosin (A, B), and DAPI (C) staining of dBECM seeded with rat MSCs (Scale bar = 100 μm).

3.2.2. Thermal analysis

DSC thermograms of the investigated samples are shown in Fig. 4. dBECM powder presented a smooth thermogram, characterized by a single endothermic transformation at 113.6 °C with a slight modification in the slope at about 75 °C. Cross-linked samples were characterized by higher transformation temperatures associated to the main endothermic peak, compared to the respective uncross-linked ones, being related to the interchain reaction induced by genipin. Specifically, the measured values were 117.2 °C and 121.0 °C for the neat and cross-linked gelatin mats, while 119.6 °C and 127.0 °C for the dBECM-gelatin and cross-linked dBECM-gelatin mats, respectively, clearly indicating that the addition of dBECM shifted this characteristic temperature. An endothermic peak was also observed for both the cross-linked samples in the range 85–95 °C, that was not clearly detected for the uncross-linked samples. Finally, a broad endothermic trace appeared around 200 °C only for uncross-linked samples. A similar result for electrospun gelatin nanofibers, collected from an acidic solution, was previously reported by Ki et al. [18], ascribing this feature to the amorphous structure of random coil conformations and to the lower contents of helical conformations.

3.3. Biocompatibility analysis

3.3.1. MSC characterization

The first adherent cells, isolated from rat bone marrow, grew as spindle- or stellate-shaped cells, and developed into visible colonies 3–5 days after the initial plating. They remained dormant for 3–5 days, then began to multiply rapidly, and reached confluence on the 8th to 10th day. The number of CFU-F was $(3.7 \pm 0.3) \times 10^5/10^6$ seeded cells. After passage 4, the adherent cells showed a uniform appearance, the expression of MSC surface antigen resulted positive for CD44, CD54, and CD90 and negative for CD11b, MHCII and GFAP (Table 1). The results confirmed that we used a homogeneus population of MSCs with no significant contamination of hematopoietic or neural (glial) cells.

3.3.2. MSC cultures on mats

Genipin cross-linked mats, both containing or not dBECM, resulted cytocompatible for *in vitro* rat MSC cultures (Fig. 5): H&E staining showed cells with a fibroblastic-like, stretched out morphology, typical for MSCs (Fig. 5A, B); while DAPI staining revealed dividing cells on dBECM-gelatin mats (Fig. 5D, inset). SEM micrographs confirmed cellular morphology and showed multilayered cell cultures, completely covering the mats (Fig. 6). H&E and DAPI staining of sectioned constructs revealed cellular growth on both sides of the mats (Fig. 7A–D), with the presence of multilayered cultures especially on the dBECM-gelatin mats (Fig. 7C–D, inset).

Flow cytometric analysis was used to evaluate antigen expression of rat MSCs cultured on genipin cross-linked mats (Table 2). The results showed a decreased expression of CD54 and a significantly ($p < 0.05$) higher expression of GFAP, specific marker for neural cells, in cells cultured on both type of mats with respect to negative controls. In particular, results showed that dBECM-gelatin mats induced a significant ($p < 0.05$) decrease in CD54 expression and the higher GFAP expression, suggesting a more effective differentiation potential towards neural (glial) pathway.

3.3.3. MNC cultures

Genipin cross-linked mats resulted cytocompatible also for *in vitro* rat MNC cultures (Fig. 8). SEM micrographs showed, especially on dBECM-gelatin mats, the presence of cells with spindle-shaped appearance, like the mesenchymal lineage, displaying membrane extensions in close contact with mat fibers, and smaller round-shaped cells similar to hematopoietic cells.

4. Discussion

Tissue engineering approach could be a key therapeutic option to repair CNS lesions and to establish a growth-promoting environment. A variety of biomaterials has been developed, such as nanofiber scaffolds [19,20], natural derived scaffolds [21–25], and hydrogels [26–28], however, to date, no clinical intervention to promote tissue regeneration after brain injury has been reported [29–31]. Several studies have highlighted that brain microenvironment has a major influence on cell proliferation and survival. In particular neuronal differentiation, migration and axon guidance are highly dependent on the interaction with the cerebral ECM [7–10,32,33], which plays a pivotal role in regulating ionic and nutritional homeostasis [34]. Replacing the lost ECM can therefore potentially supply the transplanted cells with their "natural" microenvironment and facilitate the regeneration of novel tissue [35]. In particular, the ECM derived from decellularized tissues has been successfully used to facilitate the constructive remodeling of numerous tissues and organs and it has been demonstrated that the structural and biochemical complexity of the ECM is critical in the induction of desirable healing outcomes. Moreover, it has been demonstrated that an ECM bioscaffold represents an appropriate microenvironment for neural stem

Fig. 1. *Characterization of decellularized brain matrix*. Hematoxylin and eosin (A, B), and DAPI (C, D) staining of native (A, C) and decellularized (B, D) brain. After DEM the brain matrix resulted to be completely decellularized and no cells and nuclear material were detected. Movat pentachromic (E, F) staining and SEM micrographs (G, H) of native (E, G) and decellularized (F, H) brain. Black indicates nuclei and elastic fibers; yellow collagen and reticulum fibers; and red fibrinoid, fibrin muscle. The three-dimensional architecture of brain matrix remained intact and unaltered. (I) Elastin content measurement. Elastin contents (μg/mg of total wet weight) of native and decellularized brain. (J) Sulfated glycosaminoglycan (GAG) measurement. GAG contents (μg/mg of total dry weight) of native and decellularized brain (Panels A–F: scale bar = 100 μm; Panels G, H: scale bar = 20 μm). (For interpretation of the references to colour in this figure legend, the reader is referred to the web version of this article.)

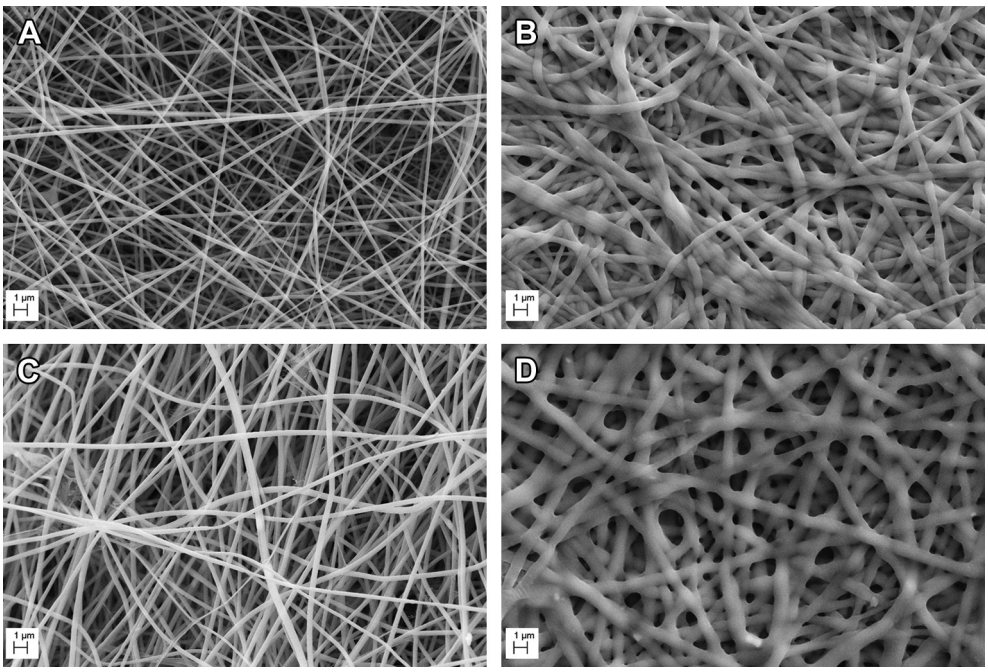

Fig. 3. SEM micrographs of as-spun gelatin (A), cross-linked (B), as-spun dBECM-gelatin (C), and cross-linked dBECM-gelatin (D) mats (Scale bar = 1 µm).

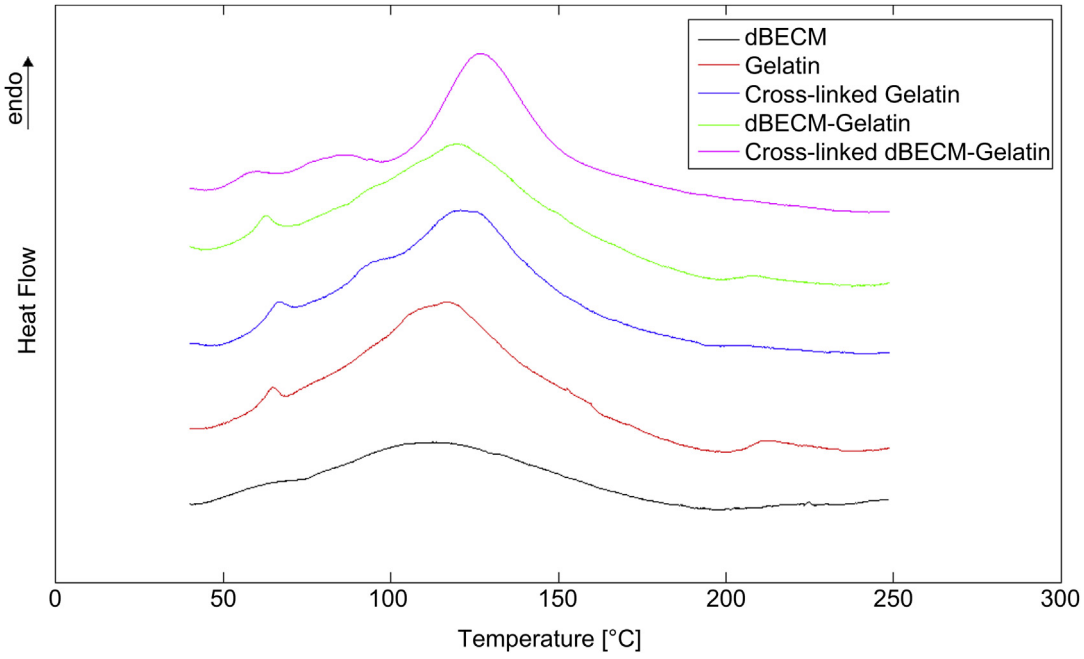

Fig. 4. DSC thermograms of dBECM, neat and dBECM-treated electrospun mats before and after genipin cross-linking.

Table 1
The expression of MSC surface antigens at passage 4.

Marker	Mean ± SD
Vitality	80 ± 3
CD 44	99 ± 3
CD 54	94 ± 5
CD 90	99 ± 4
CD11b	2.7 ± 0.2
HLA-II	Neg
GFAP	Neg

cells, promoting neurogenesis in several tissues [36–38]. There has been a clinical precedent for the application of ECM scaffolds in reconstruction of CNS structures [39,40], but this approach has till now received scarce attention and no scaffolds, which contain the appropriate tissue-specific ECM biochemical cues, have been developed for the brain [17,41–43].

The methods by which ECM scaffolds are prepared can markedly affect the composition, architecture, and material properties, and, therefore, should be carefully selected. Ribatti et al. [17], using a detergent-enzymatic method (DEM), obtained an acellular brain scaffold able to induce a strong angiogenic response. Moreover,

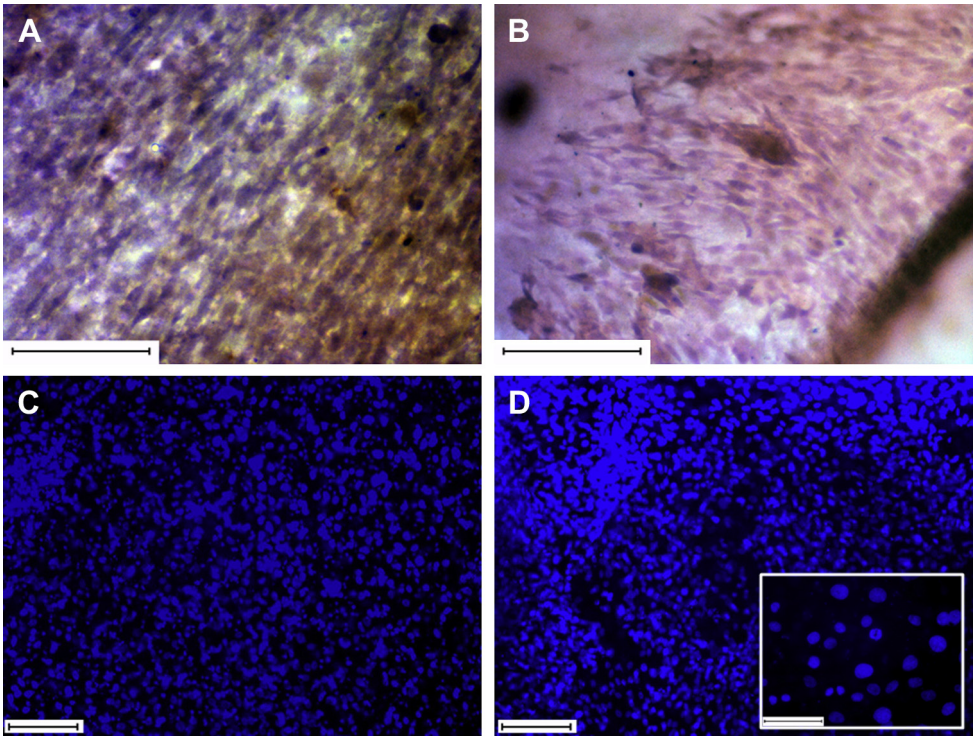

Fig. 5. Hematoxylin and eosin (A, B), and DAPI (C, D) staining of cross-linked gelatin (A, C) and cross-linked dBECM-gelatin (B, D) mats seeded with rat MSCs (Scale bar = 100 μm).

decellularized CNS matrices have been recently developed [42,43]. These studies suggest that CNS-ECM, inducing cell proliferation and differentiation into site-appropriate cells, may provide tissue-specific advantages in CNS regenerative medicine applications, aiding functional recovery after CNS injury. In this regard, the tissue-specific ECM represents a valuable means to elicit a positive biological response, especially if stem cells are used and must be guided in safe differentiation into specific lineages.

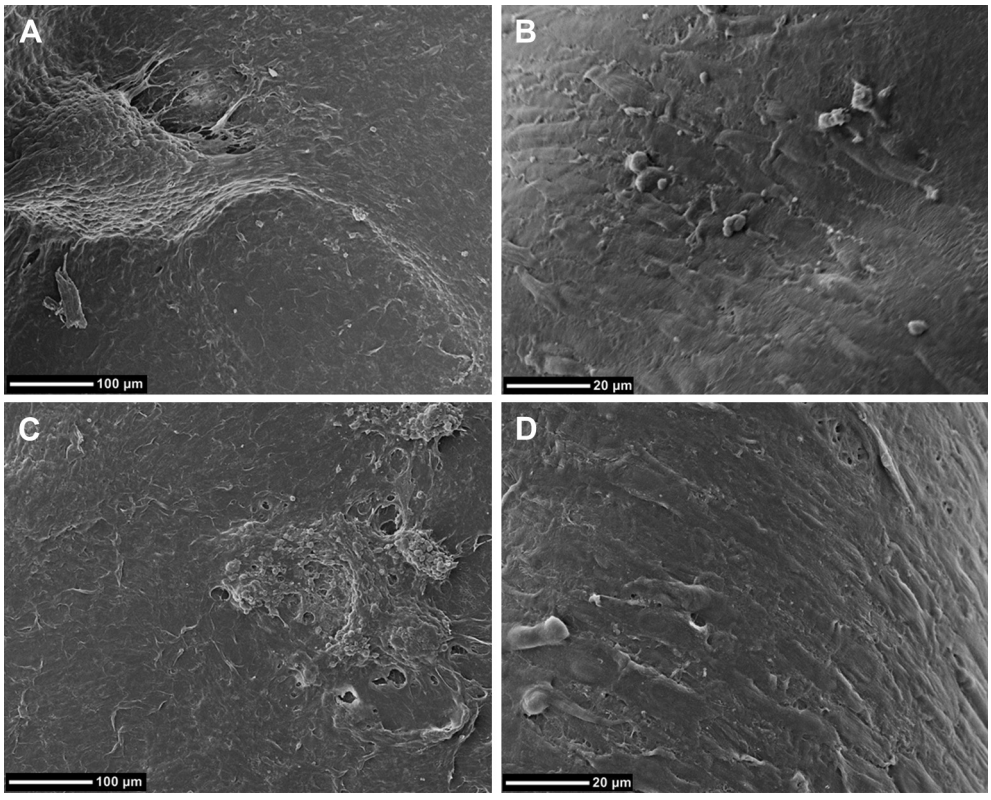

Fig. 6. SEM micrographs of cross-linked gelatin (A, C) and cross-linked dBECM-gelatin (B, D) mats seeded with rat MSCs (Scale bar = 100 μm).

In this study, we evaluated the efficacy of the previously developed DEM [17,44,45] to obtain rat brain acellular matrices. Considering that the brain lipidic composition prevents the seepage of solution into the matrix and the brain ECM is characterized by a weak structure which disrupts readily, the DEM approach has been slightly modified. Both Triton X-100 and deoxycholate were used as detergents to remove cellular content. Histological and quantitative DNA analysis demonstrated the almost complete absence of cells and cell membranes and confirmed the decellularization of brain matrix. It is well known that the structure and the composition of ECM influence cell adhesion and differentiation and provide critical physical/chemical cues that orchestrate tissue formation and function [46,47]. Our results showed that DEM did not significantly alter the morphology and histoarchitecture of brain matrix, demonstrating that the three-dimensional structure of brain ECM was well preserved. Moreover, matrix content evaluation revealed that the dBECM contained the same concentration of ECM components that are found in the native brain, suggesting that DEM process was able to retain elastin and sulfated GAGs, which have been shown to have an effect on cell behavior [48]. Finally, the presence of MSCs on both the external part and the inner core of seeded dBECM, after *in vitro* culturing, suggested that DEM approach did not damage and/or remove matrix binding sites/proteins necessary for cellular adhesion and growth. Results of decellularized rat brains demonstrated the effectiveness of modified DEM process to obtain a complete tissue decellularization, preserving ECM structural components necessary for cell attachment and repopulation.

Recent studies have demonstrated that hydrogel forms of decellularized CNS-ECM are cytocompatible, promote cell differentiation and support three-dimensional neurite extension [49]. Decellularized ECM can be electrospun, alone or in combination with polymers, in order to obtain highly porous three-dimensional scaffolds able to support cellular proliferation and differentiation [15,16]. The aim of the proposed work was the evaluation of electrospun gelatin mats incorporating decellularized rat brain tissue as a supportive platform for rat MSC and MNC adhesion and growth. The feasibility to fabricate such a scaffold was here confirmed as a one-step electrospinning procedure by adding dBECM to the polymeric solution to be processed. Moreover, considering the "precious" nature of dBECM, the ability to blend it with a natural polymer reduces the amount of starting matrix needed for fabricating a sizeable construct and improve structural properties, while maintaining the dBECM biologic relevance. In our study, a low amount of dBECM (1% w/w with respect to gelatin) was used which compares favorably with respect to the quantity needed to develop CNS-ECM hydrogels [49].

Uniform and bead-free fibers were collected, and the fibrous structure was also retained after cross-linking, even if the average fiber diameter increased. The modification of the fibrous morphology due to the cross-linking process is a common result previously verified, especially if stabilization of electrospun gelatin mats is carried out by immersion into cross-linking solutions [50]. Thermal analysis showed a specific behavior for all the investigated conditions, highlighting the influence of the genipin treatment related to an increase of the main endothermic peak temperatures.

Table 2
The expression of surface antigens on MSCs seeded onto the genipin cross-linked mats with or without dBECM (mean ± SD).

Marker	Gelatin mats	dBECM-Gelatin mats
CD 44	99 ± 1	99 ± 2
CD 54	86.2 ± 7.2	78.5 ± 1.5[a]
CD 90	92 ± 7	98.4 ± 0.4
CD11b	2.9 ± 0.4	Neg
HLA-II	Neg	Neg
GFAP	7.45 ± 0.35[a]	14.5 ± 5.5[a]

[a] $p < 0.05$ from control cultures.

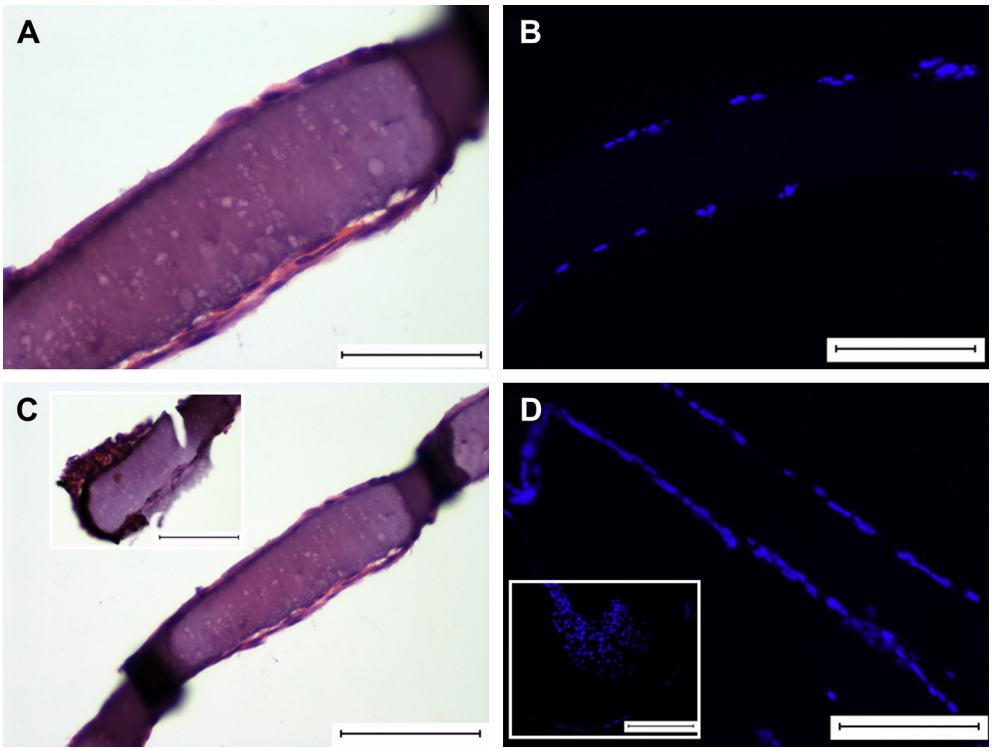

Fig. 7. Hematoxylin and eosin (A, C), and DAPI (B, D) staining of sectioned cross-linked gelatin (A, B) and cross-linked dBECM-gelatin (C, D) mats seeded with rat MSCs (Scale bar = 100 μm).

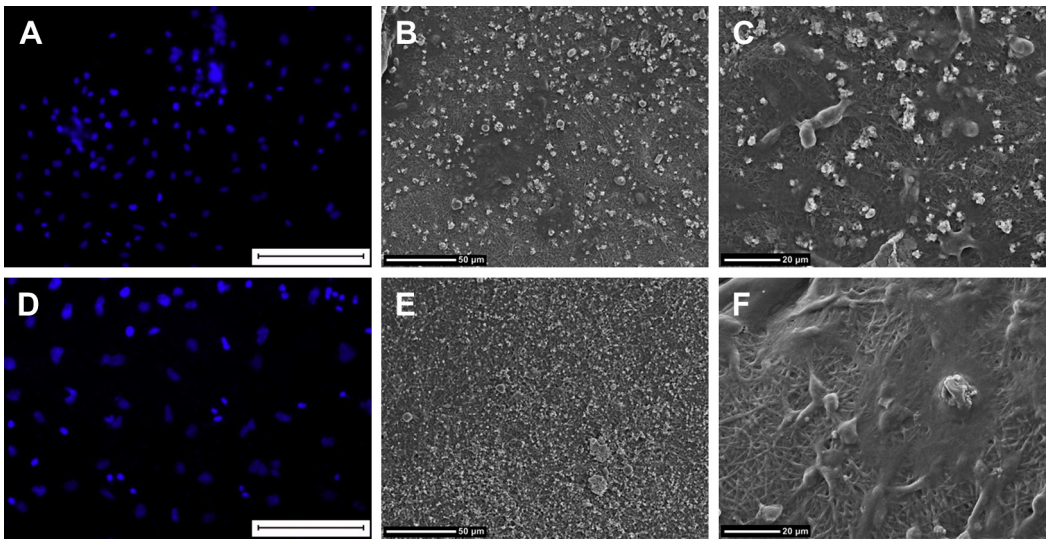

Fig. 8. DAPI (A, D) staining and SEM micrographs (B, C, E, F) of cross-linked gelatin (A–C) and cross-linked dBECM-gelatin (D–F) mats seeded with rat MNCs (Scale bar = 100 μm).

The presence of the dBECM concurred to further increase these values either before and after cross-linking, also contributing to narrow the peak of the main endothermic transformation for the latter case. This occurrence might be related to a more effective cross-linking procedure due to the addition of the brain tissue, that was also affected by genipin treatment, thus delaying the onset of the thermal transformation. Infrared spectroscopy also showed slight modifications in the spectrum of each sample, mainly due to the chemical treatment rather than to the presence of the biological matrix. In fact, the clear contribution of the dBECM in the acquired results was not directly detectable, most probably due to the presence of collagen and its similarity with the electrospun polymer (i.e., gelatin) (data not shown).

To investigate the potential of the obtained samples, rat MSCs and MNCs were cultured on genipin cross-linked mats. Cells adhered, spread and proliferated extensively in both containing or not dBECM genipin cross-linked mats, suggesting that the natural ECM protein-based mats were not cytotoxic. In particular, results revealed that dBECM-gelatin mats allowed not only cell adhesion and spreading, but also cellular proliferation and the formation of multilayered cultures.

The potential of MSCs to differentiate into cells of neuronal lineage, such as astrocytes, oligodendrocytes, and neurons, has been reported [51]; moreover, Park et al. [52] demonstrated that human MSCs cultured in hyaluronic acid-based hydrogels were able to differentiate into neural cell lineage. Analyzing the expression of a specific marker for neural cells (GFAP), we found that, after being cultured on genipin cross-linked mats, rat MCSs started to express GFAP and its expression changed depending upon the mat composition, with dBECM genipin cross-linked mats inducing a twofold higher expression. Moreover, cells seeded on dBECM genipin cross-linked mats expressed a significant reduced expression for CD54, which is not expressed in glial cells [53]. Our results suggest that the incorporation of dBECM into gelatin cross-linked mats could play a role in triggering the differentiation of MSCs to neural/glial precursor cells.

5. Conclusions

The decellularization procedure here considered, being a critical step to minimally affect the biological tissue, revealed its suitability to preserve most of the biochemical cues that contributed to the assessed cell response. This study demonstrated the potential of electrospun gelatin mats, incorporating rat decellularized brain extracellular matrix, to act as effective scaffolds providing a suitable microenvironment for mesechymal stromal cell adhesion, proliferation and survival. It was also demonstrated that the presence of the brain matrix may induce an initial stromal cell differentiation towards neural precursor cells. The collected findings can be regarded as a relevant step for the treatment for CNS affections, according to the tissue engineering paradigm. A straightforward experimental procedure was presented and its suitability to readily fabricate scaffolds with enhanced properties was proved. Since the *in vitro* evaluation showed the effectiveness of the proposed approach, future investigations may develop specific *in vivo* protocols aimed to define a neurogical therapeutic strategy.

Acknowledgments

This work was supported by a grant (pd 239-28/04/2009, GRT 1210/08) issued on the 28 December 2008 by the region Tuscany (Italy) entitled “Clinical laboratory for complex thoracic respiratory and vascular diseases and alternatives to pulmonary transplantation” and by a grant of the Government of the Russian Federation for the state support of scientific researches (agreement No. 11.G34.31.0065 dated October 19, 2011).

References

[1] Badylak SF, Weiss DJ, Caplan A, Macchiarini P. Engineered whole organs and complex tissues. Lancet 2012;379:943–52.
[2] Wang Y, Wei YT, Zu ZH, Ju RK, Guo MY, Wang XM, et al. Combination of hyaluronic acid hydrogel scaffold and PLGA microspheres for supporting survival of neural stem cells. Pharm Res 2011;28:1406–14.
[3] Olesen J, Leonardi M. The burden of brain diseases in Europe. Eur J Neurol 2003;10:471–7.
[4] Modo M, Stroemer RP, Tang E, Patel S, Hodges H. Effects of implantation site of stem cell grafts on behavioral recovery from stroke damage. Stroke 2002;33:2270–8.
[5] Lo EH, Dalkara T, Moskowitz MA. Mechanisms, challenges and opportunities in stroke. Nat Rev Neurosci 2003;4:399–415.
[6] DiProspero NA, Meiners S, Geller HM. Inflammatory cytokines interact to modulate extracellular matrix and astrocytic support of neurite outgrowth. Exp Neurol 1997;148:628–39.
[7] Zimmermann DR, Dours-Zimmermann MT. Extracellular matrix of the central nervous system: from neglect to challenge. Histochem Cell Biol 2008;130:635–53.
[8] Mai J, Fok L, Gao H, Zhang X, Poo MM. Axon initiation and growth cone turning on bound protein gradients. J Neurosci 2009;29:7450–8.

[9] Lanfer B, Hermann A, Kirsch M, Freudenberg U, Reuner U, Werner C, et al. Directed growth of adult human white matter stem cell-derived neurons on aligned fibrillar collagen. Tissue Eng Part A 2010;16:1103–13.
[10] Kwok JCF, Warren P, Fawcett JW. Chondroitin sulfate: a key molecule in the brain matrix. Int J Biochem Cell Biol 2012;44:582–6.
[11] Novak U, Kaye AH. Extracellular matrix and the brain: components and function. J Clin Neurosci 2000;7:280–90.
[12] Viapiano MS, Matthews RT. From barriers to bridges: chondroitin sulfate proteoglycans in neuropathology. Trends Mol Med 2006;12:488–96.
[13] Zhong Y, Bellamkonda RV. Biomaterials for the central nervous system. J R Soc Interface 2008;5:957–75.
[14] Francis MP, Sachs PC, Madurantakam PA, Sell SA, Elmore LW, Bowlin GL, et al. Electrospinning adipose tissue-derived extracellular matrix for adipose stem cell culture. J Biomed Mater Res A 2012;100:1716–24.
[15] Stankus JJ, Freytes DO, Badylak SF, Wagner WR. Hybrid nanofibrous scaffolds from electrospinning of a synthetic biodegradable elastomer and urinary bladder matrix. J Biomater Sci Polym Ed 2008;19:635–52.
[16] Hong Y, Huber A, Takanari K, Amoroso NJ, Hashizume R, Badylak SF, et al. Mechanical properties and in vivo behavior of a biodegradable synthetic polymer microfiber-extracellular matrix hydrogel biohybrid scaffold. Biomaterials 2011;32:3387–94.
[17] Ribatti D, Conconi MT, Nico B, Baiguera S, Corsi P, Parnigotto PP, et al. Angiogenic response induced by acellular brain scaffolds grafted onto the chick embryo chorioallantoic membrane. Brain Res 2003;989:9–15.
[18] Ki CS, Baek DH, Gang KD, Lee KH, Um IC, Park YH. Characterization of gelatin nanofiber prepared from gelatin–formic acid solution. Polymer 2005;46:5094–102.
[19] Cao H, Liu T, Chen SY. The application of nanofibrous scaffolds in neural tissue engineering. Adv Drug Deliv Rev 2009;61:1055–64.
[20] Leung GKK, Wang YC, Wu W. Peptide nanofiber scaffold for brain tissue reconstruction. Meth Enzymol 2012;508:177–90.
[21] Yannas IV. Applications of ECM analogs in surgery. J Cell Biochem 1994;56:188–91.
[22] Hsu WC, Spilker MH, Yannas IV, Rubin PA. Inhibition of conjunctival scarring and contraction by a porous collagen-glycosaminoglycan implant. Invest Ophthalmol Vis Sci 2000;41:2404–11.
[23] Harley BAC, Gibson LJ. In vivo and in vitro applications of collagen-GAG scaffolds. Chem Eng J 2008;137:102–21.
[24] Yannas IV, Tzeranis DS, Harley BA, So PT. Biologically active collagen-based scaffolds: advances in processing and characterization. Philos Transact A Math Phys Eng Sci 2010;368:2123–39.
[25] Yi X, Jin G, Tian M, Mao W, Qin J. Porous chitosan scaffold and ngf promote neuronal differentiation of neural stem cells in vitro. Neuro Endocrinol Lett 2011;32:705–10.
[26] Wei YT, Tian WM, Yu X, Cui FZ, Hou SP, Xu QY, et al. Hyaluronic acid hydrogels with IKVAV peptides for tissue repair and axonal regeneration in an injured rat brain. Biomed Mater 2007;2:S142–6.
[27] Aurand ER, Lampe KJ, Bjugstadt KB. Defining and designing polymers and hydrogels for neural tissue engineering. Neurosci Res 2012;72:199–213.
[28] Lim TC, Toh WS, Wang LS, Kurisawa M, Spector M. The effect of injectable gelatin-hydroxyphenylpropionic acid hydrogel matrices on the proliferation, migration, differentiation and oxidative stress resistance of adult neural stem cells. Biomaterials 2012;33:3446–55.
[29] Tisdall MM, Smith M. Multimodal monitoring in traumatic brain injury: current status and future directions. Br J Anaesth 2007;99:61–7.
[30] Crooks CY. Traumatic brain injury: the importance of rehabilitation and treatment. Mol Med 2008;105:140–4.
[31] Fitch MT, Silver J. CNS injury, glial scars, and inflammation: Inhibitory extracellular matrices and regeneration failure. Exp Neurol 2008;209:294–301.
[32] Rivas RJ, Burmeister DW, Goldberg DJ. Rapid effects of laminin on the growth cone. Neuron 1992;8:107–15.
[33] McKeon RJ, Jurynec MJ, Buck CR. The chondroitin sulfate proteoglycans neurocan and phosphacan are expressed by reactive astrocytes in the chronic CNS glial scar. J Neurosci 1999;19:10778–88.
[34] Rauch U. Extracellular matrix components associated with remodeling processes in brain. Cell Mol Life Sci 2004;61:2031–45.
[35] Baeten KM, Akassoglou K. Extracellular matrix and matrix receptors in blood brain barrier formation and stroke. Dev Neurobiol 2011;71:1018–39.
[36] Agrawal V, Brown BN, Beattie AJ, Gilbert TW, Badylak SF. Evidence of innervation following extracellular matrix scaffold-mediated remodelling of muscular tissues. J Tissue Eng Regen Med 2009;3:590–600.
[37] Boruch AV, Nieponice A, Qureshi IR, Gilbert TW, Badylak SF. Constructive remodeling of biologic scaffolds is dependent on early exposure to physiologic bladder filling in a canine partial cystectomy model. J Surg Res 2010;161:217–25.
[38] Bible E, Dell'Acqua F, Solanky B, Balducci A, Crapo PM, Badylak SF, et al. Non-invasive imaging of transplanted human neural stem cells and ECM scaffold remodeling in the stroke-damaged rat brain by (19)F- and diffusion-MRI. Biomaterials 2012;33:2858–71.
[39] Haq I, Cruz-Almeida Y, Siqueira EB, Norenberg M, Green BA, Levi AD. Postoperative fibrosis after surgical treatment of the porcine spinal cord: a comparison of dural substitutes. Invited submission from the Joint Section Meeting on Disorders of the Spine and Peripheral Nerves. J Neurosurg Spine March 2004;2005(2):50–4.
[40] Bejjani GK, Zabramski J. Safety and efficacy of the porcine small intestinal submucosa dural substitute: results of a prospective multicenter study and literature review. J Neurosurg 2007;106:1028–33.
[41] Guo SZ, Ren XJ, Wu B, Jiang T. Preparation of the acellular scaffold of the spinal cord and the study of biocompatibility. Spinal Cord 2010;48:576–81.
[42] DeQuach JA, Yuan SH, Goldstein LS, Christman KL. Decellularized porcine brain matrix for cell culture and tissue engineering scaffolds. Tissue Eng Part A 2011;17:2583–92.
[43] Crapo PM, Medberry CJ, Reing JE, Tottey S, van der Merwe Y, Jones KE, et al. Biologic scaffolds composed of central nervous system extracellular matrix. Biomaterials 2012;33:3539–47.
[44] Baiguera S, Jungebluth P, Burns A, Mavilia C, Haag J, De Coppi P, et al. Tissue engineered human tracheas for in vivo implantation. Biomaterials 2010;31:8931–8.
[45] Baiguera S, Gonfiotti A, Jaus M, Comin CE, Paglierani M, Del Gaudio C, et al. Development of bioengineered human larynx. Biomaterials 2011;32:4433–42.
[46] Nelson CM. Geometric control of tissue morphogenesis. Biochim Biophys Acta 2009;1793:903–10.
[47] Reilly GC, Engler AJ. Intrinsic extracellular matrix properties regulate stem cell differentiation. J Biomech 2010;43:55–62.
[48] Ushakova GA, Nikonenko IR, Nikonenko AG, Skibo GG. Extracellular matrix heparin induces alteration of the cell adhesion during brain development. Neurochem Int 2002;40:277–83.
[49] Medberry CJ, Crapo PM, Siu BF, Carruthers CA, Wolf MT, Nagarkar SP, et al. Hydrogels derived from central nervous system extracellular matrix. Biomaterials 2013;34:1033–40.
[50] Del Gaudio C, Baiguera S, Boieri M, Mazzanti B, Ribatti D, Bianco A, et al. Induction of angiogenesis using VEGF releasing genipin-crosslinked electrospun gelatin mats. Biomaterials 2013;34:7754–65.
[51] Kopen GC, Prockop DJ, Phinney DG. Marrow stromal cells migrate throughout forebrain and cerebellum, and they differentiate into astrocytes after injection into neonatal mouse brains. Proc Natl Acad Sci USA 1999;96:10711–6.
[52] Park J, Lim E, Back S, Na H, Park Y, Sun K. Nerve regeneration following spinal cord injury using matrix metalloproteinase-sensitive, hyaluronic acid-based biomimetic hydrogel scaffold containing brain-derived neurotrophic factor. J Biomed Mater Res 2012;93A:1091–9.
[53] Grau V, Herbst B, van der Meide PH, Steiniger B. Activation of microglial and endothelial cells in the rat brain after treatment with interferon-gamma in vivo. Glia 1997;19:181–9.